

# ***Pneuman*: A Humanoid Robot Implementation**

Scott Nortman  
sdn@mil.ufl.edu

Antonio Arroyo  
arroyo@mil.ufl.edu

Michael Nechyba  
nechyba@mil.ufl.edu

Eric Schwartz  
ems@mil.ufl.edu

Machine Intelligence Laboratory  
Department of Electrical and Computer Engineering  
University of Florida, Gainesville, FL 32611-6200

Florida Conference on Recent Advances in Robotics (FCRAR)  
Florida International University, Miami, Florida, May 23-24, 2002

## **Abstract**

*Humanoid robots have been popularized in science fiction for decades, but the reality is that researchers are still years away from creating an autonomous humanoid robot. Realization of such a system would have endless uses in industry, the home, assistive care, and a countless number of other areas. There are many universities and companies that are currently developing the systems needed to accomplish this difficult task, unfortunately with limited success. While progress is slow, any contribution aiding the development of humanoid systems takes us one step closer to science fiction. Therefore, the University of Florida's Machine Intelligence Laboratory is currently developing a humanoid robot as a research platform. This paper describes the development of the humanoid robot and the required control systems. Mechanical design considerations, including the forward and inverse kinematics, will be discussed. The control theory, control loop implementation, and the joint trajectory generation will also be explained in detail.*

## **1. Introduction**

The University of Florida's Machine Intelligence Laboratory (MIL) is currently developing an autonomous humanoid robot. The goal of the project is to provide the MIL with a robust humanoid research platform. The research areas of interest include artificial cognition, natural language processing, active stereo vision, path planning, autonomous navigation, inverse kinematics, manipulator control, and human-humanoid interaction. Details regarding the physical aspects of *Pneuman*, including the size of the structure, the degrees of freedom, the drive system, and the kinematics will be presented and explained in Section 2. The electronics systems will be covered in Section 3; this includes the computer system, the custom electronics, and the sensor systems. Section 4 explains the control theory and trajectory generation techniques *Pneuman* uses. A text based user interface was also developed, allowing all of *Pneuman*'s parameters to be adjusted. This will be presented in Section 5. Section 6 concludes by discussing future research.



**Fig. 1: MIL's humanoid, *Pneuman***

## **2. Physical Structure**

### **2.1 Overall Size**

*Pneuman* stands approximately 59 inches tall, measured from the bottom of the drive wheels to the top of the stereo head. The widest points are from shoulder to shoulder and across the base, both measuring 26 inches across. Each of the five DOF arms allows *Pneuman* to grasp objects approximately 20 inches away. The base consists of the lower 29 inches of the robot, while the remaining 30 inches includes the upper torso.

### **2.2 Weight**

The overall weight of the structure is a primary concern because *Pneuman* is an autonomous robot. Therefore, the power source for all electronics and actuators are carried on-board and no external power may be used. While efficient control and motor operation techniques are utilized, the best way to ensure a long battery life is to minimize the weight of the robot. The weight-minimized configuration was not conceived initially; previous plans called for a

much bulkier structure. The final revision is shown in Figure 1.

The entire robot weighs approximately 102 pounds. A major portion of the weight may be attributed to the four sealed lead acid batteries, each weighing approximately 10 pounds. *Pneuman's* base weighs approximately 25 pounds (excluding the batteries), the upper torso weighs approximately 30 pounds (including the five DOF arms), and the head weighs approximately seven pounds. Other components such as connectors and wires make up the additional weight.

### 2.3 Mobility

In terms of mobility, the goal was to give *Pneuman* access to the same areas humans live and work in. Two main locomotion options included a wheeled base or a legged walking mechanism. The wheeled base is more efficient for accomplishing a given task, and it simplifies the overall design considerably. While a legged mechanism offers some advantages over rough terrain, *Pneuman* will primarily travel over smooth surfaces. Due to these constraints, a wheeled drive base is used.

### 2.4 Degrees of Freedom

The human body has over 40 DOF. While *Pneuman* attempts to mimic the human form, simplifications were made to ensure autonomous real-time control. Therefore, *Pneuman* has 25 DOF. To accomplish the humanlike motions, two five DOF arms will be used. Each arm will have a gripper as an end-effector. In addition to the arms, *Pneuman* will have an active stereo head with three DOF, containing two cameras. Each camera may be considered an "eye." Both eyes will tilt together, while each eye can converge independently. The head will sit on a two DOF neck, allowing the entire head to pan and tilt. The entire upper torso connects to the wheeled base via a two DOF waist. The waist will allow the upper torso to tilt front to back and side to side. Finally, *Pneuman* moves via four drive wheels, each wheel steering independently, giving *Pneuman* maximum maneuverability.

### 2.5 Drive System

*Pneuman's* base contains four drive wheels arranged in a square. Each wheel is capable of steering independently, known as a modified-synchronous drive system. This gives *Pneuman* maximum maneuverability. The drive system can operate in three different steering modes; "skid-steer", Ackerman, and "four-wheel" or crab steer. While crab steering is primarily used, each has advantages and disadvantages that will be explained in later sections.

The wheels are approximately six inches in diameter and 13 inches apart. The wheels pivot about their center line and have an operating range of 180 degrees. Each wheel and steering mechanism is geared to a 485 oz.-in.

planetary gearhead motor, providing adequate torque. The maximum velocity of the motors is approximately 45 r.p.m., permitting each wheel to change steering direction at a maximum rate of  $180^\circ/1.3s$ . The given motor/wheel combination also allows *Pneuman* to translate at a maximum rate of 14 in/s.

A quantitative description of motion involves a way to describe the path of the agent and the kinematics of the mechanism required for that motion. A straight path is described by the distance traveled,  $d$ . An arc of radius  $r_s$  and a sweep angle  $\theta_s$  may describe a curved path. The kinematics may be determined from simple geometry. The *instantaneous center of curvature (I.C.C.)*, a point where the base's motion appears to move around, lies where the perpendicular bisectors of each wheel intersect with each other. Any configuration of the wheels that do not allow all of the bisectors to intersect at a common point will cause wheel slippage, resulting in inaccuracies while path planning. See Figure 2.

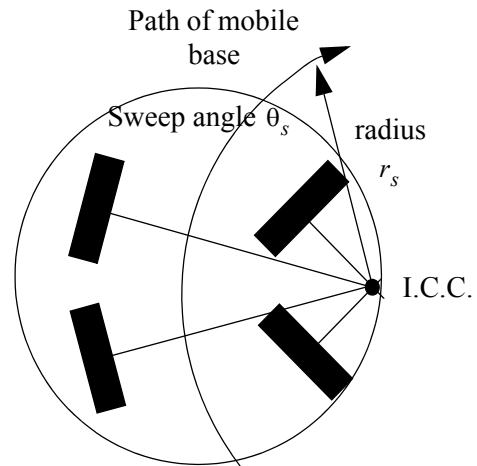


Fig. 2: The Instantaneous Center of Curvature, I.C.C.

*Pneuman* has three steering modes: skid, Ackerman, and four-wheel or "crab," and each mode will be explained in detail. Skid steering is not typically used due to inaccuracies associated with it. Ackerman steering is commonly used on automobiles, and much research has been done on the theory and modeling of this steering configuration. However, there are kinematic constraints that limit its use. The final and preferred method is four-wheel steering where all of the wheels are capable of changing their orientation. *Pneuman* will primarily use this method of steering.

### Skid Steering

Many wheeled robots use "skid steering". This simply means that the orientation of each drive wheel is fixed, and turning is made possible by varying the speed of each side's drive wheels with respect to the other side. This is an effective

tive and easy solution to steering the robot. However, it is not as accurate as other steering methods; certain characteristics including friction, wheel slippage, and other unpredictable attributes cause problems[1]. This steering configuration is a special case where the bisectors of the wheels do not intersect and the fact that the wheels slip is exploited to cause the robot to rotate. See Figure 3.

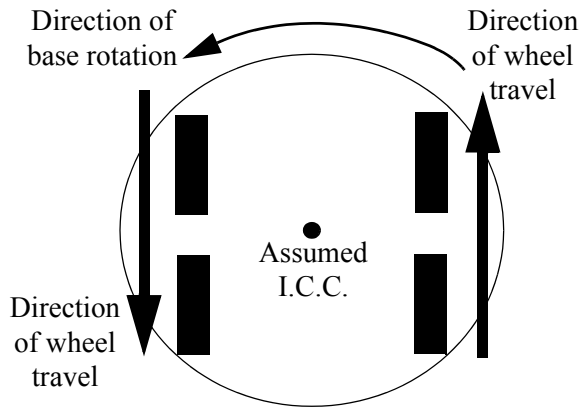


Fig. 3: Skid steering. Note the I.C.C. is assumed.

#### Ackerman Steering

Ackerman steering is used in most automobiles. The two rear wheels remain at a fixed orientation, facing towards the front of the vehicle. This means that the perpendicular bisector is the same for both rear wheels, extending in a line away from the vehicle. The two front wheels change their steering angle to steer the vehicle. Note that the steering angle for each of the front wheels is different to insure that their perpendicular bisectors intersect at the same point along the rear wheel perpendicular bisector. See Figure 4.

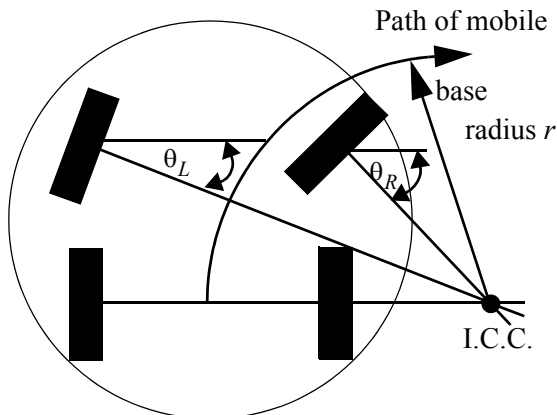


Fig. 4: Ackerman steering.

#### Four-wheel Steering

Four-wheel, or “crab” steering, has the same requirement as Ackerman steering; all of the wheel's perpendicu-

lar bisectors must intersect at a common point to avoid wheel slippage. In this mode, however, all of the wheels are allowed to change orientation. This means that the *I.C.C.* can be anywhere, not just along the mutual perpendicular of the rear wheels as in Ackerman steering. A major advantage of this mode is that the turning radius can vary from zero (about the robots center) to infinity (a straight line), and it can lie anywhere in the plane of motion. See Figure 5.

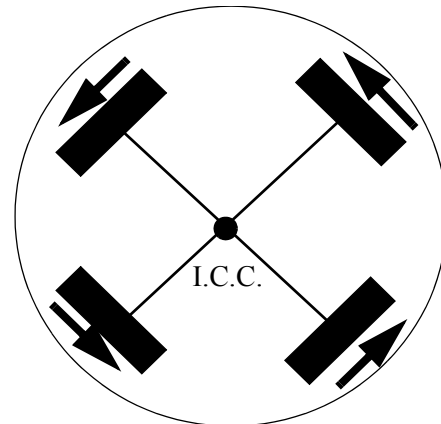


Fig. 5: Four-wheel or “crab” steering.

#### 2.6 Stereo Head

*Pneuman's* vision system consists of a three DOF stereo head with convergence, tilt, and pan. These DOF are needed to allow *Pneuman* identify the location of an object in a 3D space. Each eye can move independently, allowing each camera to converge on to an object. Additionally, each eye uses an optical encoder providing an angular resolution of 0.036 degrees. This will allow *Pneuman* to determine the location of objects with high accuracy.

#### 2.7 Robotic Arms

The details regarding the design and kinematic of the two robotic arms are discussed in Nortman et al, 2001. See Figure 6 for a CAD rendering of an arm.



Fig. 6: One of *Pneuman's* robotic arms.

## 2.8 Waist Assembly

The waist joint kinematics must be considered in addition to the head, neck, and arm kinematics. The waist is a two DOF joint, exactly like a universal joint, providing *Pneuman's* upper torso pitch and yaw movement. As in the arm design, both axes of rotation are aligned to keep the kinematics simple. See Figure 7 for a kinematic representation of the waist joint and placement of the reference frames.

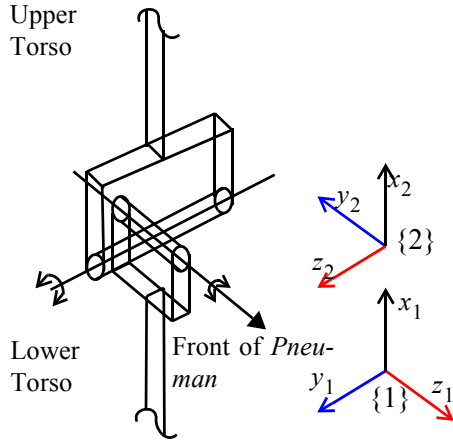


Fig. 7: Kinematic diagram of waist assembly.

The closed-form forward and inverse kinematic solution to the waist joint is given by the following set of equations:

$${}^0_2T = \begin{bmatrix} r_{11} & r_{12} & r_{13} & p_x \\ r_{21} & r_{22} & r_{23} & p_y \\ r_{31} & r_{32} & r_{33} & p_z \\ 0 & 0 & 0 & 1 \end{bmatrix} \quad (1)$$

$${}^0_2T = \begin{bmatrix} \cos(\theta_1)\cos(\theta_2) & -\cos(\theta_1)\sin(\theta_2) & -\sin(\theta_1) & 0 \\ \cos(\theta_2)\sin(\theta_1) & -\sin(\theta_1)\sin(\theta_2) & \cos(\theta_1) & 0 \\ -\sin(\theta_2) & -\cos(\theta_2) & 0 & 0 \\ 0 & 0 & 0 & 1 \end{bmatrix} \quad (2)$$

$$\theta_1 = \text{atan2}(-r_{13}, r_{23}) \quad (3)$$

$$\theta_2 = \text{atan2}(-r_{31}, -r_{32}) \quad (4)$$

## 3. Electronic Systems

A block diagram of the electronic systems found on *Pneuman* is shown in Figure 8. For a detailed discussion of the electronic and control systems, see Nortman et al, 2001.

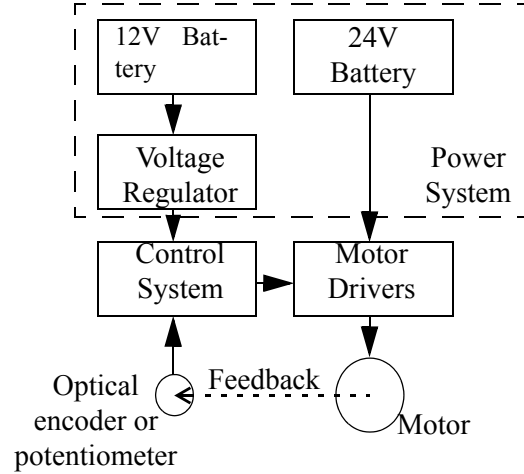


Fig. 8: *Pneuman's* electronics and control systems.

## 4. Control Theory

### 4.1 Overview

*Pneuman's* mechanical structure has 25 DOF. Each DOF is actuated by a direct current (DC) motor and has a sensor for feedback. The embedded computer analyzes the information from the sensor and controls the corresponding DC motor to achieve the desired output. Each DOF, with its own DC motor and sensor, constitutes a closed loop system. There are two different types of sensors used on *Pneuman*; potentiometers provide absolute joint position for 19 of the 25 DOF and incremental optical encoders are used on the drive wheels and stereo head. The details regarding the use of each sensor will be discussed in sections 4.2 and 4.3.

Although a control system provides a way to achieve a desired output, the ways to determine what the desired output should be are also considered. For example, if a particular joint is positioned at 0 degrees and the desired position is 90 degrees, how should the joint move from the initial to the final position? Do you simply command the controller to position the joint at 90 degrees as fast as possible? Will that cause too much mechanical strain on the joint? What if you wanted it to move "smoothly" over a period of 5 seconds? These issues will also be discussed in detail.

### 4.2 Analog Feedback Control

Nineteen of *Pneuman's* joints use analog potentiometers for feedback. They operate as absolute position encoders, providing a voltage reference indicating the joint angle. This voltage signal is fed into an analog to digital converter, providing eight-bits of resolution over the potentiometer's operational range of 300 degrees. Therefore, each bit corresponds to 1.17 degrees of movement, which is an ac-

ceptable resolution for *Pneuman's* designated purpose as an experimental research platform.

All of the joints utilizing a potentiometer use a discrete approximation of the proportional, derivative, and integral (PID) control law, with gravity compensation (except for the steering mechanisms), implemented in software. This robust control law was selected due to its simplicity and good performance. The discrete PID controller is implemented with equation 4-4:

$$\begin{aligned} \mu(n) = & k_P \cdot e(n) + k_I \sum_{n=0}^N e(n) \\ & + k_D[e(n) - e(n-1)] \end{aligned} \quad (5)$$

where  $\mu(n)$  is the motor control signal output, updated at the sampling time  $n$ ,  $k_P$  is the proportional gain,  $k_I$  is the integral gain,  $k_D$  is the derivative gain, and  $e(n)$  is the position error at the sample time  $n$ . All of the joints have the same sampling rate of 100 Hz, and all of the gains are individually tuned for maximum performance.

The potentiometers used as joint angle sensors may have nonlinear characteristics. For example, the potentiometer may physically rotate 90 degrees, but due to the nonlinear characteristics the analog value does not indicate a change of 90 degrees. See Figure 9.

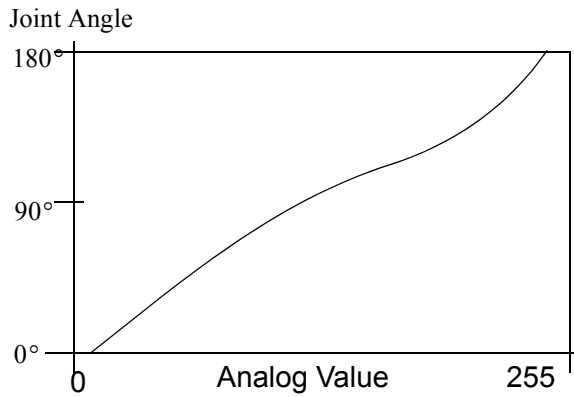


Fig. 9: Plot of uncalibrated potentiometer.

Therefore, all of the joints must be calibrated to get the most accurate measurements possible. Ideally, a large data set collected over the complete range of motion should be collected and used for an accurate calibration. However, collecting data over the complete range of motion for each DOF is not feasible due to difficulties in obtaining accurate position measurements without sophisticated tools. For this reason, three data points are collected and used to calibrate each joint.

The three data points form two lines; the slopes and y-axis intercepts of each line are the calibration parameters for each DOF. The slopes and intercepts are determined from the following equations:

$$\begin{aligned} \text{slope}_A &= \frac{\Delta \text{Joint Position}}{\Delta \text{Analog Value}} \\ &= \frac{\text{Position 1} - \text{Position 0}}{\text{Analog 1} - \text{Analog 0}} \end{aligned} \quad (6)$$

$$\begin{aligned} \text{slope}_B &= \frac{\Delta \text{Joint Position}}{\Delta \text{Analog Value}} \\ &= \frac{\text{Position 2} - \text{Position 1}}{\text{Analog 2} - \text{Analog 1}} \end{aligned} \quad (7)$$

$$\text{Intercept A} = \text{Position 1} - (\text{slope}_A \cdot \text{Analog 1}) \quad (8)$$

$$\text{Intercept B} = \text{Position 1} - (\text{slope}_B \cdot \text{Analog 1}) \quad (9)$$

For example, each drive wheel is calibrated at -90, 0, and +90. The corresponding analog values are recorded and used to calibrate the joint. The calculated calibration lines are then used to interpolate joint position between the calibration points. See Figure 10.

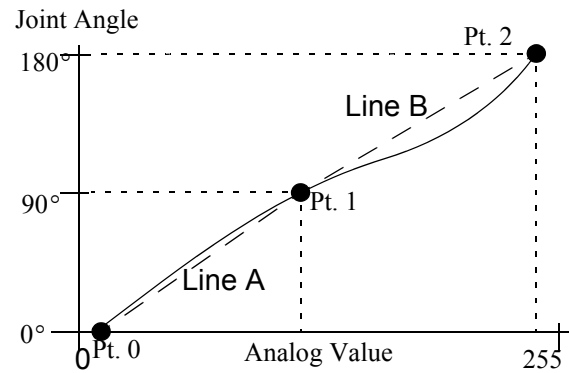


Fig. 10: Calibrated potentiometer plot.

### 4.3 Digital Feedback Control

*Pneuman's* drive wheels and stereo head actuators each use incremental optical encoders for feedback. These non-contact sensors permit a full 360 degrees of rotation, a requirement for the drive wheels. The wheel encoders have a resolution of 0.18, allowing for precision distance measurement. The stereo head convergence optical encoders have a resolution of 0.036, which is needed for precision stereo vision. Each of the encoders connects to a National Semiconductor LM629 motion control integrated circuit (IC). This specialty-purpose controller interfaces directly to an optical encoder and outputs a signed-magnitude PWM signal for motor control.

The LM629 is a specialty purpose micro controller which interfaces directly to a quadrature optical encoder for feedback. *Pneuman's* main computer issues commands to the LM629 via the pc/104 bus, and the IC generates the desired motion trajectory. The PID filter is given by the equation

$$\mu(n) = k_P \cdot e(n) + k_I \sum_{n=0}^N e(n) + k_D[e(n') - e(n' - 1)] \quad (10)$$

where  $\mu(n)$  is the motor control signal output, updated at the sampling time  $n$ ,  $e(n)$  is the position error at the sample time  $n$ ,  $n'$  indicates the derivative sampling rate,  $k_P$  is the proportional gain,  $k_I$  is the integral gain, and  $k_D$  is the derivative gain[3].

The desired overall motions of a manipulator may be considered a multidimensional trajectory, which is a history of position, velocity and acceleration versus time. While a qualitative description of a trajectory appears trivial (i.e., make the end-effector go from point A to point B), a quantitative description is more difficult. Questions such as, ‘‘How fast should the manipulator move?’’ and, ‘‘What if there is an obstacle in the way?’’ need to be addressed. Even though a quantitative description is not trivial to compute, an end user of a robotic system should not have to deal with all details of the desired motions. Instead, a goal position and orientation may be given and the control system calculates the best way to get there.

There are a number of ways to move a robot from point A to point B, but they all share a common attribute; they allow the robot to move ‘‘smoothly.’’ A motion may be considered smooth if it is continuous and differentiable. This type of motion decreases wear on the mechanics, reduces vibrations, and generally improves the performance of a manipulator.

Calculating a smooth trajectory requires that some constraints be placed on the paths between the points along a trajectory. These constraints guarantee a smooth path will be executed:

$$\theta(0) = \theta_0 \quad (11)$$

$$\theta(t_f) = \theta_f \quad (12)$$

$$\dot{\theta}(0) = 0 \quad (13)$$

$$\dot{\theta}(t_f) = 0 \quad (14)$$

These equations indicate that the starting position at time  $t = 0$  is  $\theta_0$ ,  $\theta_f$  is the final position at  $t_f$ . and the starting and ending velocities are zero.

These four constraints necessitate a function with four coefficients, a cubic polynomial. A cubic polynomial has the following form:

$$\theta(t) = a_0 + a_1 t + a_2 t^2 + a_3 t^3 \quad (15)$$

with velocity and acceleration given by:

$$\dot{\theta}(t) = a_1 + 2a_2 t + 3a_3 t^2 \quad (16)$$

$$\ddot{\theta}(t) = 2a_2 + 6a_3 t \quad (17)$$

Solving for the four cubic coefficients we get

$$a_0 = \theta_0 \quad (18)$$

$$a_1 = 0 \quad (19)$$

$$a_2 = \frac{3}{t_f^2}(\theta_f - \theta_0) \quad (20)$$

$$a_3 = -\frac{2}{t_f^3}(\theta_f - \theta_0) \quad (21)$$

where  $\theta_0$  is the initial position,  $\theta_f$  is the final position, and  $t_f$  is the amount of time allotted to complete the trajectory [4].

The trajectories of *Pneuman's* drive wheels are determined using this method. This simple trajectory generation scheme was chosen because the steering assembly does not require additional constraints on the velocities and accelerations. The amount of time required to execute any given trajectory is determined by taking the ratio of the desired movement over the overall range of motion and multiplying by the time allowed for the full range of motion:

$$t_{allotted} = \frac{\Delta\theta_{given}}{\theta_{total}} \cdot t_{total} \quad (22)$$

with  $\theta_{total}$  and  $t_{total}$  varying for the different joints. The steering joints all use 180 degrees and 3 seconds, respectively.

If intermediate *via points* are needed where the velocities are not zero, the cubic coefficients are determined by:

$$a_0 = \theta_0, \quad (23)$$

$$a_1 = \dot{\theta}_0, \quad (24)$$

$$a_2 = \frac{3}{t_f^2}(\theta_f - \theta_0) - \frac{2}{t_f}\dot{\theta}_0 - \frac{1}{t_f}\dot{\theta}_f, \quad (25)$$

$$a_3 = -\frac{2}{t_f^3}(\theta_f - \theta_0) + \frac{1}{t_f^2}(\dot{\theta}_f + \dot{\theta}_0), \quad (26)$$

where  $\theta_0$  is the starting position,  $\dot{\theta}_0$  is the starting velocity,  $\theta_f$  is the final position, and  $\dot{\theta}_f$  is the final velocity of the segment.

The steering and drive assemblies do not use this technique for trajectory generation, however the rest of *Pneuman's* joints benefit from the ability to use via points. See Figure 11 for a cubic trajectory without via points and Figure 12 for a cubic trajectory with via points; the first segment from -45 degrees to 30 degrees occurs in 1.5 seconds with a via point

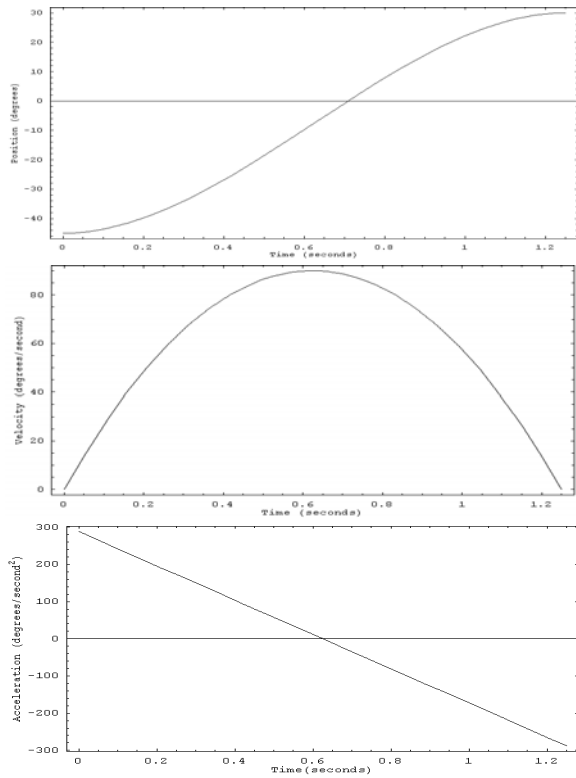


Fig. 11: Cubic trajectory without via points.

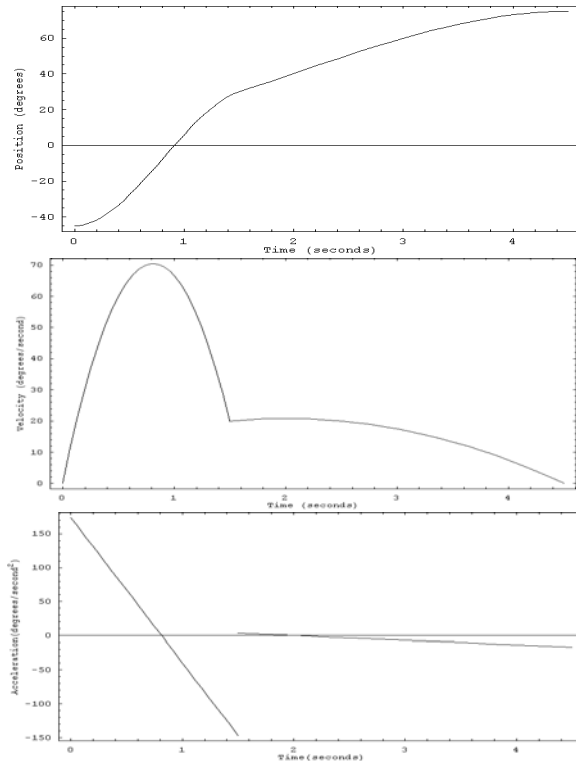


Fig. 12: Cubic trajectory with via points.

velocity of 20 degrees/second, and the second segment from 30 to 75 degrees occurs in 3 seconds with an ending velocity of 0 degrees/second [4].

## 5. User Interface

Eventually, *Pneuman* will operate autonomously. However, this is not the case during development. The user requires control over all of *Pneuman's* parameters to insure that the robot functions properly. Therefore, a text user interface is currently under development. This interface allows all of *Pneuman's* joint parameters to be calibrated, adjusted, and controlled. The initial startup screen allows the user to select a parameters menu or a control menu.

The parameters menu shows all of the attributes for all of *Pneuman's* DOF. The control loop parameters are *actual position*, *desired position*, *minimum position*, *maximum position*, *default position*, *kp*, *ki*, *kd*, and *duty cycle*. Note that the *duty cycle* can not be displayed for the LM629 control loops because it is implemented in hardware. All of the user adjusted attributes can be set from this menu. Each option may be selected by pressing the appropriate key, identified as a capital letter on the menu bar at the top of the program window.

For example, the “S” key is pressed to set the desired position of a joint. After the initial key press, a sub-window appears allowing the user to select the particular joint. Once the joint is selected, a window appears asking for a new desired position. See Figure 13.

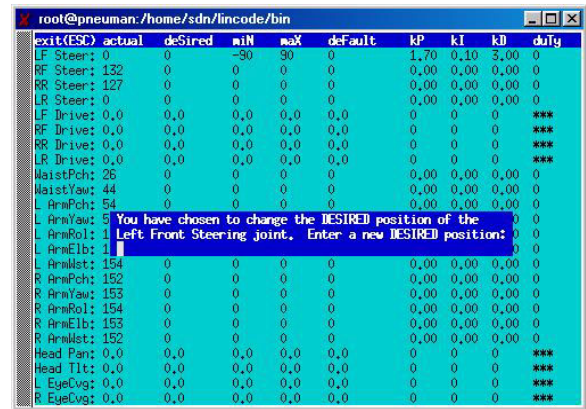


Fig. 13: Parameter screen to change a desired value.

After a desired value is entered, the joint moves to the desired position. Upon finishing the move, a real time plot of the desired trajectory, actual trajectory, and trajectory error is printed to the screen. This real-time plot is useful for determining the appropriate gains for the joints. See Figure 14.

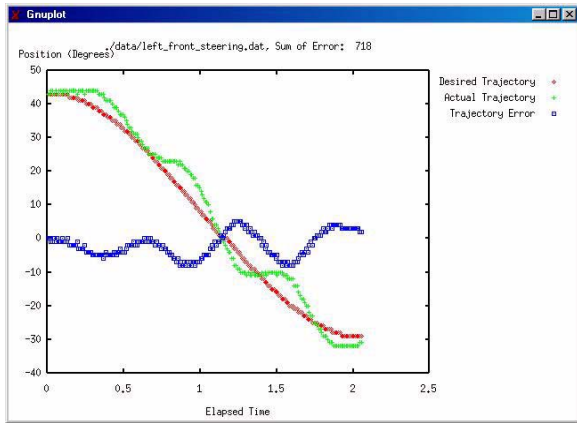


Fig. 14: Real-time trajectory plot.

## 6. Conclusion

### 6.1 Future Work

The research and development of *Pneuman* and the humanoid systems will be an ongoing project at the MIL. Before significant humanoid specific research can be accomplished, all of the underlying control and sensor systems must be implemented. This includes the control systems for the dual five DOF arms, the waist assembly, the neck assembly, and the active stereo head. The sensor systems may include the machine vision system, obstacle avoidance systems, voice recognition systems, and navigation systems.

The objectives of *Pneuman's* control systems are to move the joints in the manner specified by the trajectory generation module. This is accomplished adequately by using a PID control law, but there are still errors between the desired and actual trajectories. These errors may be attributed to inaccuracies with the feedback sensors, the dynamic models, friction, or a number of other non-modelled factors. Machine learning techniques may be used to reduce the error between the desired and actual trajectories. A proposed scheme is illustrated in Figure 15. This scheme augments the current control system with a *trainable* module. Data may be collected during execution of trajectories and used to train the module. The module will “learn” the errors in the untrained system and compensate for them, thereby reducing the error in the augmented system [5].

### 6.2 Summary

Upon researching the state-of-the-art humanoids, it is clear that we are at the very beginning of our science fiction fantasies. The most mechanically advanced self-contained humanoid, the Honda *P3*, is primarily programmed[6]. Scenes on television of this robot walking down stairs and opening doors may have led some to believe that we are

close the realization of science fiction. However, laymen do not know that millions of dollars have been spent to achieve this goal. They do not know that there were hundreds of engineers and scientists who programmed every move the robot made. They do not know that the robot did not think about walking down the stair or opening the door. It was explicitly told to move each foot, bend each knee, and rotate the elbow joint. The robot has no idea of what stairs or doors *are*. In spite of these illusions, this is the most advanced humanoid robot to date.

Currently, *Pneuman* is not as advanced as *P3*. However, they both are ideal tools for humanoid research and the current state-of-the-art will continue to move forward as companies and universities further their knowledge of the subject. Together, these research platform will help turn science fiction into science reality.

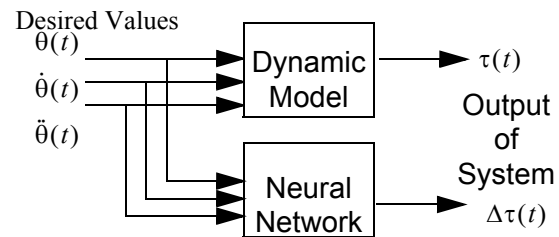


Fig. 15: Augmented control system.

## 7. References

- [1] Jones J.; Flynn A., *Mobile Robots Inspiration to Implementation*, A K Peters, Ltd., Massachusetts, 1993.
- [2] Nortman, S.; Peach, J.; Nechyba, M.; Brown, L.; Arroyo, A., “Construction and Kinematic Analysis of an Anthropomorphic Mobile Robot”, Proceedings of the 2001 Florida Conference on Recent Advances in Robotics, Volume 7, Pages 32-42.
- [3] National Semiconductor Corporation, “LM628/LM629 Precision Motion Controller”, product datasheet, 11/01/1999, <http://www.national.com/ds/LM/LM629.pdf>, accessed 9/20/2000.
- [4] Craig, J., *Introduction to Robotics: Mechanics and Control*, 2nd Edition, Addison-Wesley, Publishing Company Inc., Reading, Massachusetts, 1989.
- [5] Nechyba, M., EEL 6935 Machine Learning II, *Neural Networks and Their Applications*, Class Notes, Fall 2001.
- [6] Hirai, K.; Hirose, M.; Haikawa, Y.; Takenaka, T., “The Development of Honda Humanoid Robot”, Proceedings of the 1998 IEEE International Conference on Robotics and Automation, 1998, Volume 2, Pages: 1321-1326.